Systematic Convergence in Applying Variational Method to Double-Well Potential

Wai-Ning Mei

Department of Physics
University of Nebraska at Omaha
Omaha, Nebraska 68182
United States
physmei@unomaha.edu

(Received: 24.10.2016, Accepted: 01.11.2016)

DOI: 10.20308/ejpe.04084

Abstract
In this work, we demonstrate the application of the variational method by computing the ground- and first-excited state energies of a double-well potential. We start with the proper choice of the trial wave functions using optimized parameters, and notice that accurate expectation values in excellent agreement with the numerical results can be aquired by cautious systematic improvement of trial wave functions.
Keywords: Double-well potential, computation method, variational method.

INTRODUCTION

In this paper, we focus on employing the frequently taught variational principle (Griffiths, 2005) to compute the ground- and first-excited state energy levels of a simple symmetric, double-well potential which has extensive applications in a wide range of different areas of physics mostly in systems with degenerate ground states: from field theory to atomic, molecular physics, and consdensed matter physics (Keung, Kovac, & Sukhatme, 1988. Hardy & Flocken, 1988. DeMille, 2015).

First, the present approach is stated in many renowned quantum mechanics textbooks (Schiff, 1968. Merzabacher, 1961. Cohen-Tannoudji, Diu, & Lolöe, 1977): that is the ground state energy E_{gs} of a system can be calculated from using any trial wave function ψ_{trial} which will always be greater than the true total ground state energy E_{true} and will be equal only when we happen to choose the correct wave function. In fact, this principle can be extended to the excited states, provided the trial wave functions are orthogonal to the ground-state and excited-state wave functions (Griffiths, 2005. Mei, 1996, 1997, 1998, & 1999. Ninemire & Mei, 2004) determined previously. It is understood that when applying the method, we first calculate the total energy E_{tot} from a trial wave function, and then minimize it to obtain the best set of parameters: this is achieved by differentiating the total energy with respect to each variational parameter, and solving the resultant system of simultaneous nonlinear equations by using the numerical software packages, such as Maple or Mathematica. Next we substitute the optimized parameters back to deduce the total energy. So it is clear that the variational method is straightforward to implement, yet it is not strongly emphasized in several commonly adopted textbooks mentioned earlier: at the start, the principle is stated in a forthright manner, followed by examples with known solutions, but rarely is a

whole chapter developed on the subject as the textbook of Griffiths (2005), hence many students are not aware of its importance and practical applications.

Actually, accomplishing good results when applying the variational method hinges primarily on a clever choice of the trial wave functions suited to the problem: this depends on good physical insight and mathematical skills in evaluating the expectation values. It is important to choose a reliable wave function that reflects the true nature of the problem, which can be manipulated analytically renders the lengthy numerical computation can be reduced as much as possible. Successful examples of applying this method in the areas of molecular and condensed matter physics are abundant in the last several decades, not only is their agreement with the experimental results impeccable, but those novel methods developed also guide us into deeper understanding of the systems studied and the ideas gained extend into new areas of physics. Thus we should encourage students to familiarize with the method and let them know that will enrich their training. Here are a few renowned examples: Heitler and London's (1927) pioneer study on H_2 molecule revealed the concept of valence bonding; the Bardeen-Copper-Schrieffer (BCS) (1957) theory of superconductivity, based on a set of ingeniously constructed electron-pair wave functions, provided us with the full knowledge of the ground-state properties and excitation spectrum; Feynman's approach to the superfluid helium (1953. Feynman & Cohen, 1956), with the introduction of the correlated basis wave functions and quantum statistical mechanics arguments, directed us to understand the mechanism and energy-excitation spectrum; and the polaron problem (Feynman, 1955), with the application of the path-integral formulation that taught us to tackle the electron-phonon systems with different ranges of coupling strength. Techniques developed from these landmarks are still used in today's mainstream research. Despite advancement in numerical simulation and computation techniques, there are still exciting problems require insights and analytical mathematical techniques to unravel, such as investigating the strong correlation effects in Hubbard model (Gutzwiller, 1965), integer and fractional quantum Hall effects (Laughlin, 1981, 1983), novel trial wave-functions are constructed to verify different intriguing scenarios. Thus in this work we emphasize on teaching of the variational method during quantum mechanics classes: by providing more interesting example for practice, our students will learn the method and be encouraged to apply it in the real situations. For many years, the prowess of the variational method was demonstrated by several groups of my students in their research projects (Hedgahl, Johnson III, Schnell, & Ward, 2008. Koch, Schuck, & Wacker, B, 2008). They found the experience rewarding for developing their research careers, because the numerical software packages relieved them from lengthy computations and enable them to focus on constructing the trial wave-functions and analyzing results.

In many cases, solving numerically Schrödinger equation with a particular model potential is time-consuming and the solutions are not easy to implement. This is why many other approximation techniques, such as the Wentzel-Kramers-Brillouin (WKB) approximation method, are taught in the above-mentioned commonly adopted undergraduate textbooks and have been shown to be of great use in finding bound states and elucidating tunneling effects. However, the double-well potential bound-state energies are hard to calculate when the well depth increases. Indeed known numerical integration techniques can provide accurate energies, but the tabulated numerical wave functions are difficult to utilize. Only in rare cases are there a few specifically constructed double-well potentials for which their one-dimensional Schrödinger equations can be solved analytically (Manning, 1935. Razavy, 1979): the first one was used to simulate the energy spectra of molecules like NH_3, and the other provides solutions to explain diffusion phenomena described by the Fokker-Planck equation. Yet in both cases the potentials and their solutions are composed of hyperbolic functions which are not easy to extend to other problems. Thus, in most cases a simplified potential $V(z)=z^4-\gamma z^2$ composed of a postive quartic and negative quadratic term, where γ is a postive constant, is used to illustrate the essential degenerate nature of this potential: i.e. there are two equivalent minima located at $z_{min}=\pm\sqrt{\frac{g}{2}}$ with depth $V_{min}=-\frac{g^2}{4}$. So when γ increases, the two minima separate further apart, the potential becomes deeper, and the lowest two energies get closer.

Consequently, one of our purposes is to study tunneling effect between the symmetric ground- and antisymmetric first excited-state that is one of the important quantum-mechanical feature of the double-well potential V(z), which is one of the simplest models able to demonstrate this effect. Particularly it becomes evident when a particle having energy much lower than the central maximum is not restricted to either one of the wells but allowed to move back and forth between the two equivalent potential minima. After comparing different methods, we recognize that it is more conveniently to extract physics insight from examining the optimized trial ground- and first-excited wave functions than replying on numerical methods, the analysis will be shown in discussion section.

Generally the tunneling rate through the double-well barrier depends strongly on the energy difference $\Delta E=E_1-E_0$ between the lowest two energies E_0 and E_1 (Keung, Kovac, & Sukhatme, 1988. Hardy & Flocken, 1988). Hence it is interesting to investigate the lowest two energies of a very deep double-well potential that is when they appear as a nearby pair. Thus our main goal is to compute separately the ground and first-excited state energies and their wave functions of the one-dimensional Schrödinger equation, first, by expressing the solutions in terms of Heun's infinite-series (Ronveaux, 1995. Slavyanov & Lay, 2000), then adopt Maple or Mathematica computer software packages, in which those special Heun functions are programmed, to compute the lowest two energies and wave functions for different values of γ. Afterward we use those computed values to compare with those acquired from using the variational method stated in Griffiths (2005), Mei (1996, 1997, 1998, & 1999), and Ninemire & Mei (2004). Our purpose is to show, with proper choice of trial functions composed of optimized parameters, not only can we generate results with high accuracy in comparison with the numerically-calculated energies, but also we obtain analytical wave functions that can be utilized for further computations.

Theoretical Background

Solution of the dimensionless Schrödinger equation with the double-well potential V(z)

$$-\frac{d^2\Psi}{dz^2}+\left(z^4-\gamma z^2\right)\Psi=\varepsilon\Psi \tag{1}$$

can be expressed in terms of a linear combination of two linearly independent Heun triconfluent functions, such as HeunT_1, and HeunT_2 which can be expressed in the form of infinite series and denoted as H_1 and H_2, respectively (Ronveaux, 1995. Slavyanov & Lay, 2000) ,

$$\Psi(z,\gamma,\varepsilon)=C_1H_1(z,\gamma,\varepsilon)+C_2H_2(z,\gamma,\varepsilon) \tag{2}$$

Both of them are complex functions of the scaled variable z, parameter γ, and eigenvalue ε. For general eigenvalues ε, they have different asymptotic behaviors: one of them reaches zero when $z\to\infty$ and diverge as $z\to-\infty$, while the other behaves the opposite. C_1 and C_2 are two arbitrary constants to be determined from the boundary conditions. Hence for the bound-state solutions, we require $\Psi(z, \gamma, \varepsilon)\to 0$ as $z\to\pm\infty$.

To ascertain numerical solutions, we replace infinity by a finite range $\pm R$. We found the first few wave functions of simple harmonic and anharmonic oscillator potentials (Mei, 1997) approach nearly zero around R=4-5. Thus we increase R gradually and notice the roots of the following determinant derived from the asymptotice conditions reach convergent values,

$$\begin{vmatrix} H_1(R,\gamma,\varepsilon) & H_2(R,\gamma,\varepsilon) \\ H_1(-R,\gamma,\varepsilon) & H_2(-R,\gamma,\varepsilon) \end{vmatrix} = 0 \qquad (3)$$

So we regard R=5 as the proper cutoff and compute ε by solving the above determinant equation numerically with give □. We found H_1 and H_2 numerically huge and oscillatory, thus we have to describe them with a large number of digits, roughly from 40 to 80, depending on the asymptotic conditions to assure their convergence rendering the computation of Eqn. (3) reliable. We also found that when crossing zeroes of Eqn. (3), its imaginary part is extremely small and real part changes sign abruptly. In this work, we only compute the first two eigenenergies and use them to plot the wave functions. Results such as energies obtained from both the numerical and variational methods will be shown later for various γ. Finally, this way of deducing ground- and first-excited state energies using Heun functions was not achieved by any of the previously numerical schemes, as far as we know.

At first glance, the double-well potential resembles a superposition of two separated simple harmonic-oscillator potentials, thus the simplest ground state trial wave function □ground for this potential is a linear combination of two-displaced normalized Gaussian functions as follows:

$$\Psi_{ground}(z) = \frac{1}{\sqrt{2}}\left[\Psi_R(z) + \Psi_L(z)\right], \qquad (4)$$

where

$$\Psi_R(z) = \sqrt{\frac{\lambda}{\sqrt{\pi}}}e^{-\frac{\lambda^2}{2}(z-a)^2} \quad \text{and} \quad \Psi_L(z) = \sqrt{\frac{\lambda}{\sqrt{\pi}}}e^{-\frac{\lambda^2}{2}(z+a)^2}. \qquad (5)$$

□R(z) and □L(z) are the two harmonic oscillator wave functions located at the right- and left-hand side potential wells, a and λ are the parameters governing the location and shape of the wave functions. Nevertheless we notice the above assertion was accurate only when γ is small as shown in Figures 2a and 3a. Then a serious discrepancy grew as γ became larger that appeared in Figures 2b, 2c, 3b, and 3c. Thus, we have to modify the trial wave functions by including more relevant terms, which is a common practice when applying variational method and was introduced by Hylleraas (1929, 1970) to calculate the ground state energy of the He atom. The procedure became complicated when there are more terms, but the results agreed fully with experiments. After few trials, we discovered that by adding higher even-parity excited states of the harmonic oscillator wave functions we were able to achieve the purpose for the following reasons: first, the higher excited state wave functions spread wider than the ground state, hence the improved trial wave functions simulate well the behaviors in the barrier regions; second, it is known that the additional terms are orthogonal to each other, that simplifies the normalization and expectation value calculations; and third, by adding even-parity excited state components we preserve the symmetry of the ground state: i.e. □R(z) = □L(-z).

Now we designate them as the group A trial wave function, the right-hand side component is:

$$\Psi_R^A(z) = \sum_{n=0}^{N} d_n \psi_{2n}(\lambda, z-a), \qquad (6)$$

where this wave function component situated at the right-hand side of the origin with distance a, λ describing the width of the peak, and d_n is the coefficient. Notice it is summing over all the higher even-parity excited states □2n(□,z), which is the 2n-th excited state of the one-dimensional harmonic oscillator.

Similarly the left-hand side component is expressed as

$$Y_L^A(z) = \sum_{n=0}^{N} d_n y_{2n}(\lambda, z+a), \tag{7}$$

Thus a, λ, and all the d_n's are the adjustable parameters, and they can be determined from normalizing the trial wave functions and optimizing the total energy. Actually, all the overlap integrals and matrix elements of the harmonic oscillator wave functions are not difficult to evaluate, yet it becomes laborious when n is large. Fortunately, we can rely on computer algebra packages mentioned earlier, to calculate all the integrals analytically, afterward optimize the total energy by using the numerical routines to solve the system of simultaneous equations.

Then we construct the group B trial wave functions by relaxing the restriction that the parameters a and λ of all the □□□ components are the same, their right- and left-hand side components are given as:

$$Y_R^B(z) = \sum_{n=0}^{N} d_n y_{2n}(\lambda_n, z-a_n) \tag{8}$$

and,

$$Y_L^B(z) = \sum_{n=0}^{N} d_n y_{2n}(\lambda_n, z+a_n) \tag{9}$$

That is, in every new term □$_n$ there are additional parameters a_n and □$_n$ have to optimize, Hence we might not have to include as many terms as we did in the group A trial wave functions, but the optimization procedures and the overlap integrals are much more complicated than those of the group A. The maximum number of variational parameters we reached is 14: that is, the maximum n is 24 or total 13 terms for group A trial wave functions, and maximum n is 8 or total 5 terms for the group B. From Eqns. (6) to (9), we conveniently assign d_0=1.

After the ground state, we find that it is easy to extend the previous work to mimic the first excited state with a slight modification: that is, we express the variational wave function of the first excited state as:

$$Y_{excited}(z) = \frac{1}{\sqrt{2}}\left[Y_R(z) - Y_L(z)\right]. \tag{10}$$

It is easy to show the above wave function is odd, that is □$_{excited}$ (-z) = -□$_{excited}$ (z), and always orthogonal to □$_{ground}$ (z) of Eqn. (4), as long as □$_R$(z) and □$_L$(z) remain the same parity as described from Eqns. (4) to (7). Hence, we can compute the first excited state energies in a similar way. There is another advantage in constructing the first excited state as Eqn. (10): when □ gets larger, the energy difference between the two lowest states gets to be small Figure 1. Therefore it is difficult to distinguish the two adjacent roots when solving Eqn. (3). However, we can calculate the ground- and first-excited state energies separately by using those trial wave functions, Eqns. (4) and (10), thus an accurate energy difference can be achieved.

Finally, we present a quantitative way to judge the merit of our trial wave function □$_{trial}$(z): that is, we compare the true potential V(z) with the effective potential V_{eff} (Figures 2 to 6) defined as:

$$V_{eff} = E_{tot} + \frac{d^2Y_{trial}/dz^2}{Y_{trial}}, \tag{11}$$

Hence when there is discrepancy, we know what to improve and if the effective potential V_{eff} matches perfectly with the true potential V(z), this implies the trial wave function $\psi_{trial}(z)$ agrees well with the exact solution.

Discussion of Results

In this work, we present two sets of carefully constructed trial wave functions to simulate the ground- and first-excited states of a simple double-well potential $V(z)=z^4-\gamma z^2$. Following a series of systematic improvements, we were able to reach highly accurate energy expectation values. In this section, we discuss our results and the interesting phenomena encountered.

To conduct our numerical calculations, we set the parameter γ to 3, 6, and 9: first, when γ=3 (the so-called "shallow well"), the ground- and first-excited state energy levels are slightly below and above V=0, Figure1b. For γ=6 ("intermediate well"), there is only one pair of states situated at the potential well below V=0, Figure 1c. Then when γ=9 ("deep well"), more than one pair of states are located in the potential well and the lowest pair is located close to the bottom (Figure 1d). When γ changes from 3 to 9, we find ΔE decreases from 0.97 to 2.28×10^{-4}. To compare the energies obtained with those computed from the variational method, these are listed in Tables 1 and 2. Before inspecting the variational results, we observe a general feature: when using the variational method it is in general easier to reach good accuracy in the first excited-state energy than attaining the same for the ground-state energy, we attribute that to their symmetric properties: we know the ground state and first excited state of an one-dimensional symmetric potential is either even or odd parity. Hence there exists at least one point, the nodal point at z=0, in the first excited state wave functions we are sure of, due to its antisymmetry, whereas we only know that the ground-state wave functions have no node.

We start with the simplest two-term variational wave functions and notice that the numerical energies obtained only deviate a few percent from the numerical results (Tables 1 and 2). But the effective potential V_{eff} calculated by using those simplest trial wave functions are less than acceptable: for γ=3, the effective potential V_{eff} is a good fit for the true double-well potential V(z) (Figures 2a and 3a) and the spike located at z=0 is much less prominent than those of the γ=6 (Figures 2b and 3b) and γ=9 (Figures 2c and 3c). We attribute this two-term trial wave function could not simultaneously describe the behaviors at the central region, because both the width z_{min} and depth V_{min} increase when γ progresses from 3 to 9. We regard these high-rise peaks as lack of treating properly the tunneling between two deep valleys, hence we have to modify the assertion that when γ increases the ground state wave function reduces to a simple superposition of two isolated harmonic oscillator ground state wave functions. In order to help the eyes, we multiply all the wave functions in Figures 2 to 6 with a factor of 20 or 30.

To reduce those sharp spikes, we find it effective to add more even-parity higher-order harmonic oscillator excited states into the trial wave functions, because of: first, the extents of an excited state is larger than that of the ground state and so it embodies more reliable information near the origin; and second, it ensures the overall symmetry of the trial wave functions and orthogonality with each additional component. Thus starting from γ=3, we add about 6-8 even-parity excited-state components to the variational wave functions and find that the ground and first-excited state energies gradually converge to the numerical values, and the coefficients d_n get rather small for large n. When we reach 12 additional terms in the group A wave functions, the calculated expectation values match well with the numerical results, i.e. the agreement is good up to 9 to 10 significant figures, and the contributions from those addition terms are small. However, as we change γ to 6 and 9, we notice the agreement improves when higher excited state components become more important than those of the lower ones, that is, the higher n coefficients d_n are larger than those of smaller n. For example, as γ=6 in the 14-parameter optimized ground state wave function, we find that the first five coefficients are of a similar order of magnitude: among them d_1 and d_2 are slightly larger, that is $d_1/d_0 \sim d_2/d_0 \sim 2$, $d_3/d_0 \sim d_4/d_0 \sim 1$, and the rest, d_5–d_{12}, are comparatively small. But when γ=9, we notice the first four coefficients in the lengthiest optimized ground

state wave function are much larger than the others, but fairly different from the previous case, namely d_2/d_0~7, d_1/d_0~d_3/d_0~5, and all the others, d_4–d_{12}, are at least one order of magnitude smaller than those previous four coefficients, d_0–d_3. Interesting behaviors also appear when we examine the results obtained from using group B wave functions where the a_n and $\square_{\square}$ parameters of each additional terms are different: for example, in the cases of γ=6 and 9, i.e. when z_{min}~1.73–2.12. Here are our observations: (I) When γ=6, z_{min}~ 1.73, we find we find a_0~1.4, but $\square_2$ and $\square_4$ are situated near the origin, i.e. a_1~0.71, a_2~1.63, and a_3~0.62, but with small and opposite signs in d_1 and d_2, i.e. d_1~0.62, d_2~ -0.21 and d_3~0.18. (II) When γ=9, z_{min}~ 2.12, we find a_0~2.3, and $\square_2$ and $\square_4$ behave the same for in (I), i.e. a_1~0.6, a_2~1.4, and a_3~0.74, but with small and opposite signs in d_1 and d_2, i.e. d_1~0.72, d_2~ -0.34 and d_3~0.89. Also, the parameters $\square_n$ are of the similar magnitude, ~1.6–1.8, for all the $\square_{2n}$'s. Therefore, we realize that when the potential wells get deeper and separated apart, the ground state wave function contains more higher excited states components of the single harmonic oscillator potential with larger weights, which supports our earlier statements that these high excited state components provide better description to the wave functions in the central barrier region and tunneling between the two deep valleys. Incidentally, the above-mentioned features occur only in the ground state wave functions, the excited state wave functions behaved normally: d_0 maintaining the largest and all the higher-order term coefficients decrease monotonically. When optimizing the total energy, we would like to emphasize: first, it is quick to obtain the optimized total energies and variational parameters when there are only few terms in the trial wave functions. Yet when γ=6 and 9, we detect there are several competing local minima, which have similar values but different sets of parameters. Then we have to exercise great care by adding few more terms and searching the neighborhoods of different parameter spaces until one of them reaches the lowest expectation value. When adding up to 12 terms, we noticed the real minima agree well with the numerical values, Tables. 1 and 2, and the calculated effective potentials V_{eff} match exactly with the true potential V(z) (Figures 4 to 6).

When using group B trial wave functions, the restriction that all the higher excited state components should be orthogonal to each other is relaxed, there are less components but more variational parameters than those of group A. For γ=3, we notice that group A trial wave functions has a much better rate of convergence than that of group B. In general, the difference between the group A and numerical solutions are orders of magnitude smaller than those of group B when there are very few parameters. Next we change γ to 6, we see that the ground states of both groups A and B wave functions have the similar rates of convergence, especially in the ground state, whereas in the first excited state, the difference between group A and the numerical solutions are of two orders of magnitudes smaller than those of group B with the same number of parameters. Then for γ=9, we found that the ground state energies calculated using group B wave functions converge faster than those from the group A. Yet the first excited state energies calculated using group B are still more accurate than those of group A. Finally, we notice that groups A and B variational wave functions containing up to 14 parameters matched well with each other and agreed with numerical solutions composed of Heun functions deposited in large files. Also we present next to each other the optimized ground and first excited state wave functions of groups A and B together with their effective potentials and their right- and left-hand side components. Thus from comparing the wave functions in (a) to (b) and (c) to (d) from Figures 4 to 6, we realize that even though the groups A and B total wave functions agreed fully, but their right- and left-hand side components that manifest overlapping between two valleys are not remotely the same, then recognize the tunneling rate change as γ gets larger, this is another advantage that just using the numerical method can achieve.

CONCLUSIONS

In conclusion, we have demonstrated that the variational approach, when comparing to solving numerically the original differential equations, is effective in attaining accurate results and extracting physics insight. Namely, the optimized trial wave functions of group A and B containing up to 14 parameters can be used to calculate nearly analytically the matrix elements, results derived match closely with those computed from utilizing numerical Heun infinite-series solutions that require large files to

store, and include more detail features for us to examine, which we believe will constitute a good example to teach solving time-independent Schrödinger equation by using variational method.

In this work, we verify systematically that by adding more terms to the two well-thought out trial wave functions that were originally composed of displaced harmonic oscillator ground states, when determining the ground- and first excited-state energies and wave functions of the double-well potential. The variational results approach gradually with impressive accuracy, 8 to 9 significant figures, to the numerical solutions and the wave functions obtained are convenient to use. Furthermore, we have extended our calculations to 4 and 12 additional terms in the A and B groups with total 14 parameters, yet we believe more accurate results for large □ cases can be accomplished by including extra terms in the trial wave functions and furnished with more powerful computation facilities. Again, we would like to reiterate our goal of this work: advocate for teaching of the variational method in quantum mechanics classes. As mentioned in the Introduction, we implement the idea when teaching the subject by proposing a topic and guide the students through the entire process, thus the students can learn the method and get a publication at the end. Based on our experience, they found this arrangement useful for their training and research careers. Finally, we prepare all the Maple worksheets for the interested reviewers and readers to evaluate our work, please send requests to the attached addresses.

ACKNOWLEDGEMENTS

I would like to thank Professors Yung-Chang Lee, Daniel Wilkins, Wai-Yee Keung, and Renat Sabirianov for their assistances on choosing the trial wave functions and revising the manuscript. Most importantly, I am grateful for the constant and invaluable supports from Maplesoft technical consultants.

Figures

Figure 1. (a) Double-well potentials V(x) for γ=3 (black), 6 (red), and 9 (blue) together with the two lowest energy levels: ground state (green) and first excited state (brown). Magnified portions of potential V(x) (black) and those energy levels are shown in (b) γ=3, (c) γ=6, and (d) γ=9. Notice the difference in scale.

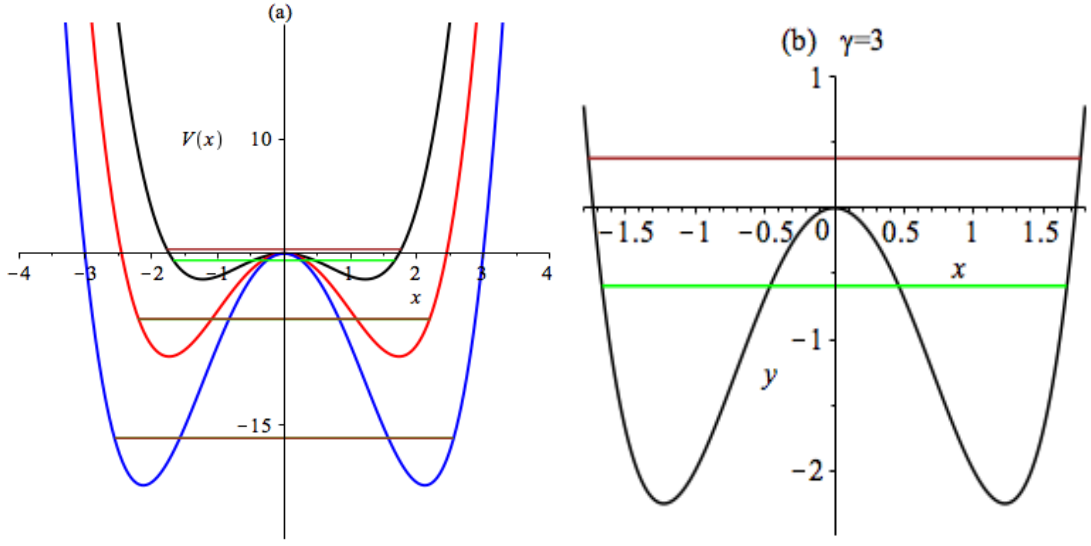

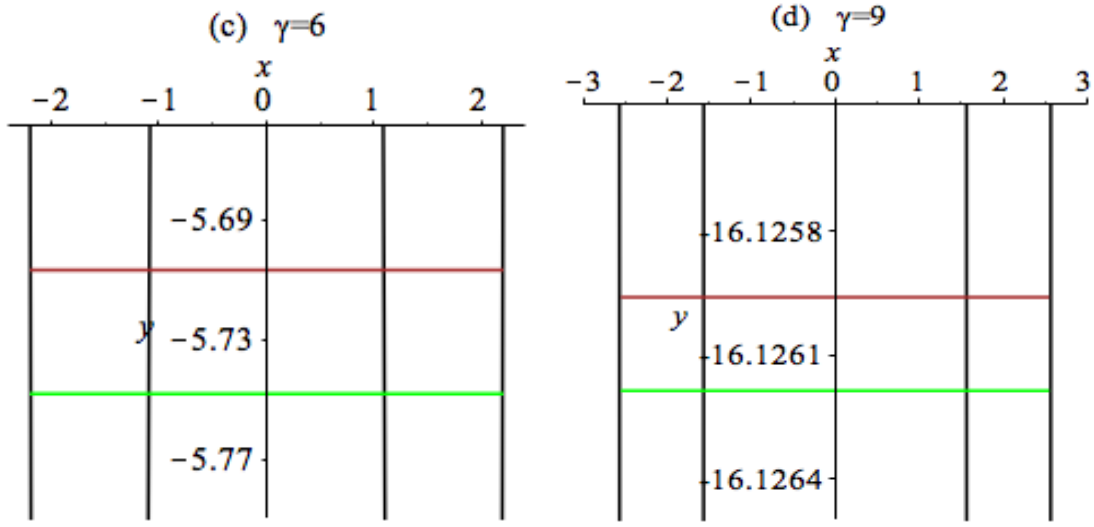

Figure 2. *Double-well potential V(z) (blue), the two-term optimized ground state wave function* $\psi_{ground}(z)$*, (Eqn. (4), x30, magenta), the effective potential* $V_{eff}(z)$ *(red) calculated by using* $\psi_{ground}(z)$*, and the difference* $(V_{eff}(z) - V(z))$ *(green), for (a)* $\gamma=3$*, (b)* $\gamma=6$*, and (c)* $\gamma=9$*.*

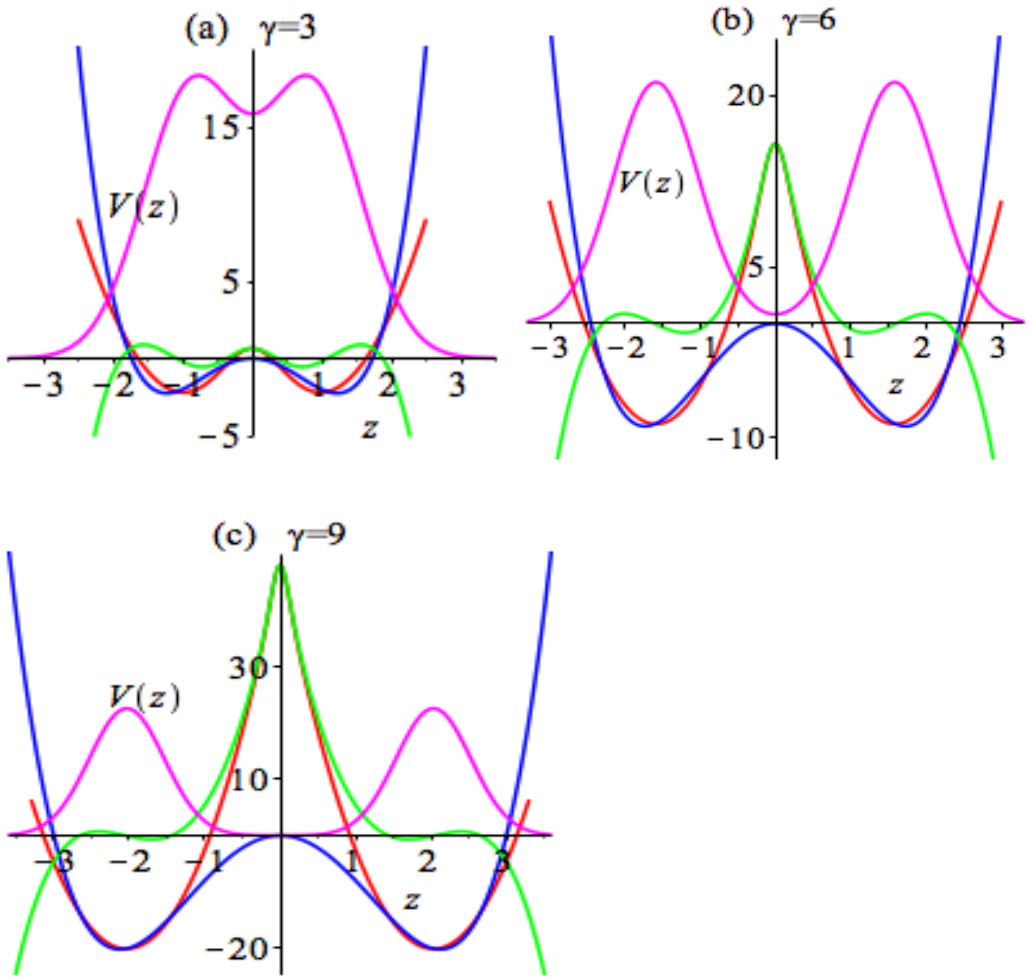

Figure 3. *Double-well potential V(z) (blue), the two-term optimized first excited state wave function* $\psi_{excited}(z)$, *(Eqn. (10), x30, magenta), the effective potential* $V_{eff}(z)$ *(red) calculated by using* $\psi_{excited}(z)$, *and the difference* $(V_{eff}(z) - V(z))$ *(green), for (a)* $\gamma=3$, *(b)* $\gamma=6$, *and (c)* $\gamma=9$.

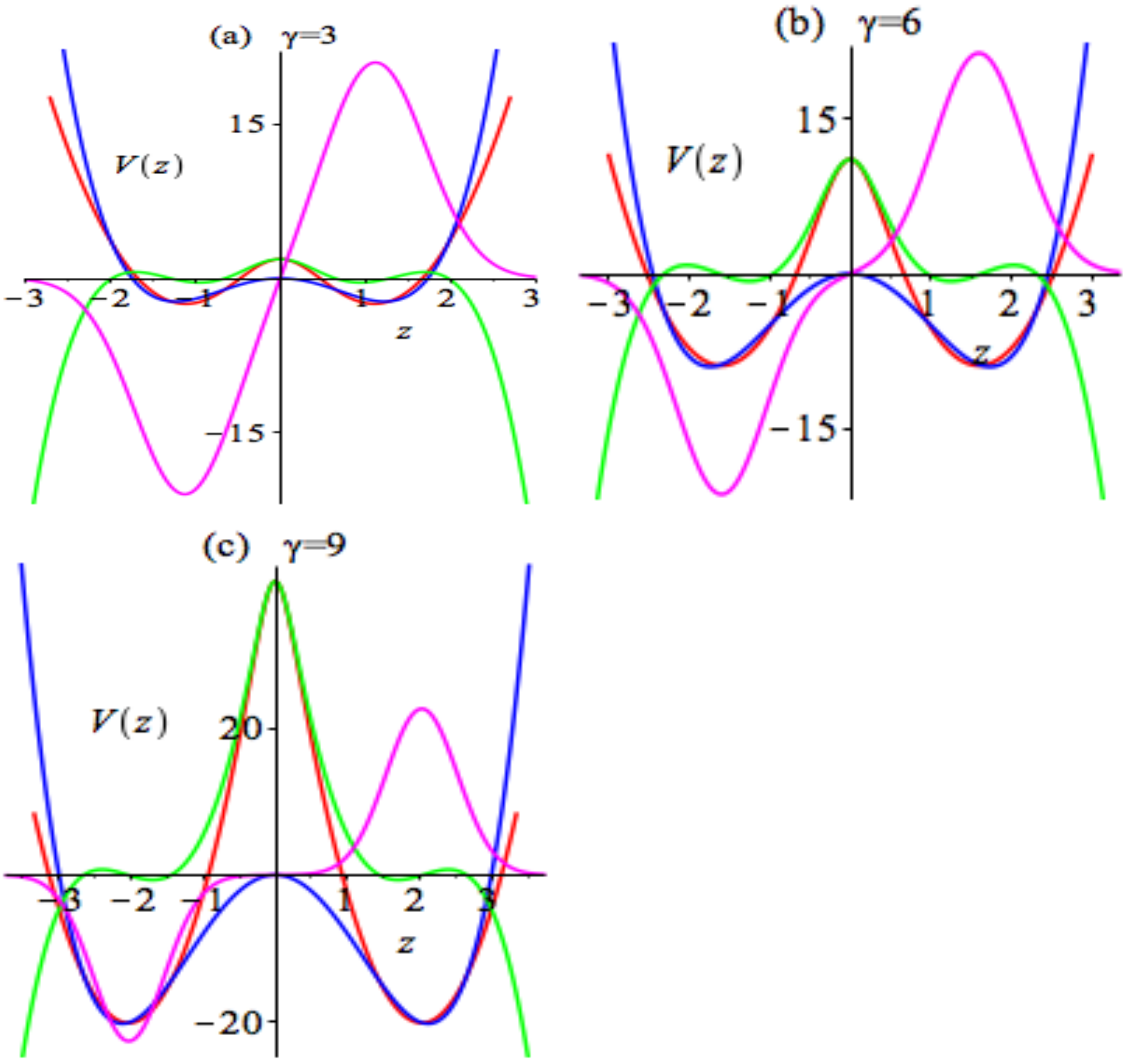

Figure 4. *Double-well potential V(z) (blue), the 14-parameter optimized wave functions* $\psi(z)$ *(x30, magenta) and the right- and left-side components (x20, brown), the effective potential* $V_{eff}(z)$ *(red) calculated by using* $\psi(z)$, *and the difference* $(V_{eff}(z) - V(z))$ *(green) for* $\gamma=3$. *(a) and (b) are the ground states of groups A and B, (c) and (d) are the first excited states of groups A and B, respectively.*

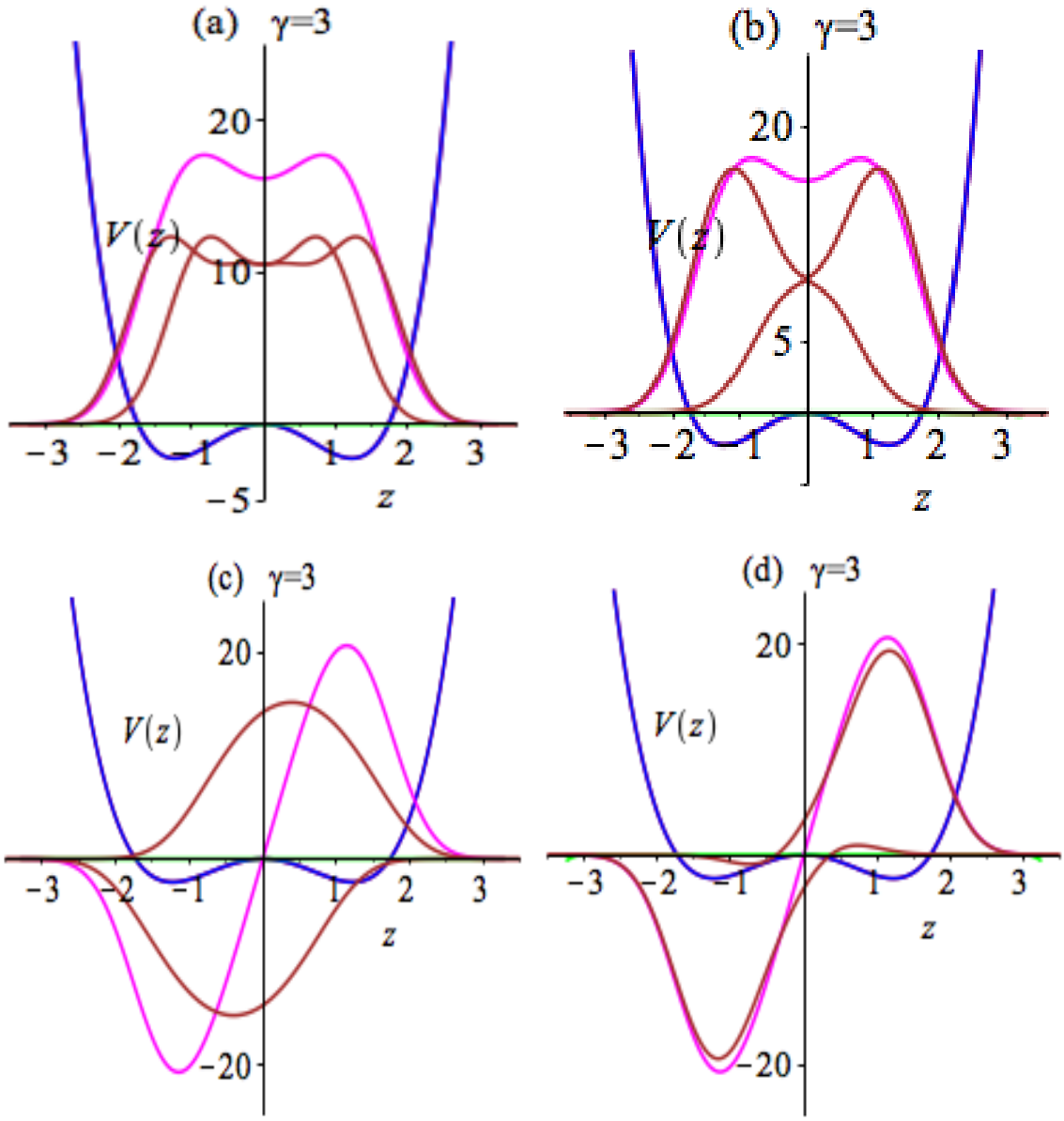

Figure 5. *Double-well potential V(z) (blue), the 14-parameter optimized wave functions □□(z) (x30, magenta) and their the right- and left-side components (x20, brown), the effective potential V_{eff}(z) (red) calculated by using □(z), and the difference (V_{eff}(z) -V(z)) (green) for γ=6. (a) and (b) are the ground states of groups A and B, (c) and (d) are the first excited states of groups A and B, respectively.*

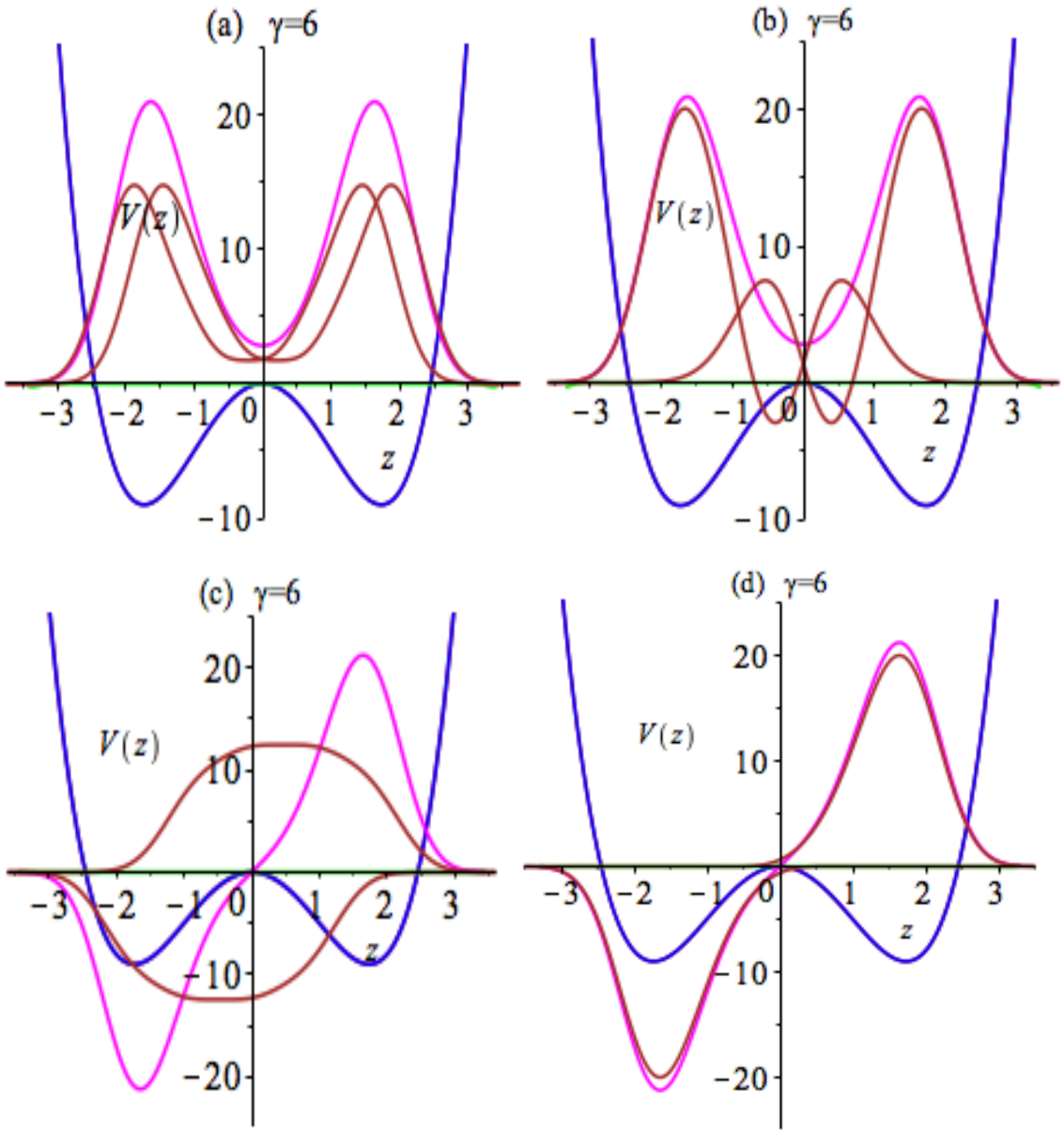

Figure 6. *Double-well potential V(z) (blue), the 14-parameter optimized wave functions □(z), (x30, magenta) and their the right- and left-side components (x20, brown), the effective potential V_{eff}(z) (red) calculated by using □(z), and the difference (V_{eff}(z) -V(z)) (green) for γ=9. (a) and (b) are the ground states of groups A and B, (c) and (d) are the first excited states of groups A and B, respectively.*

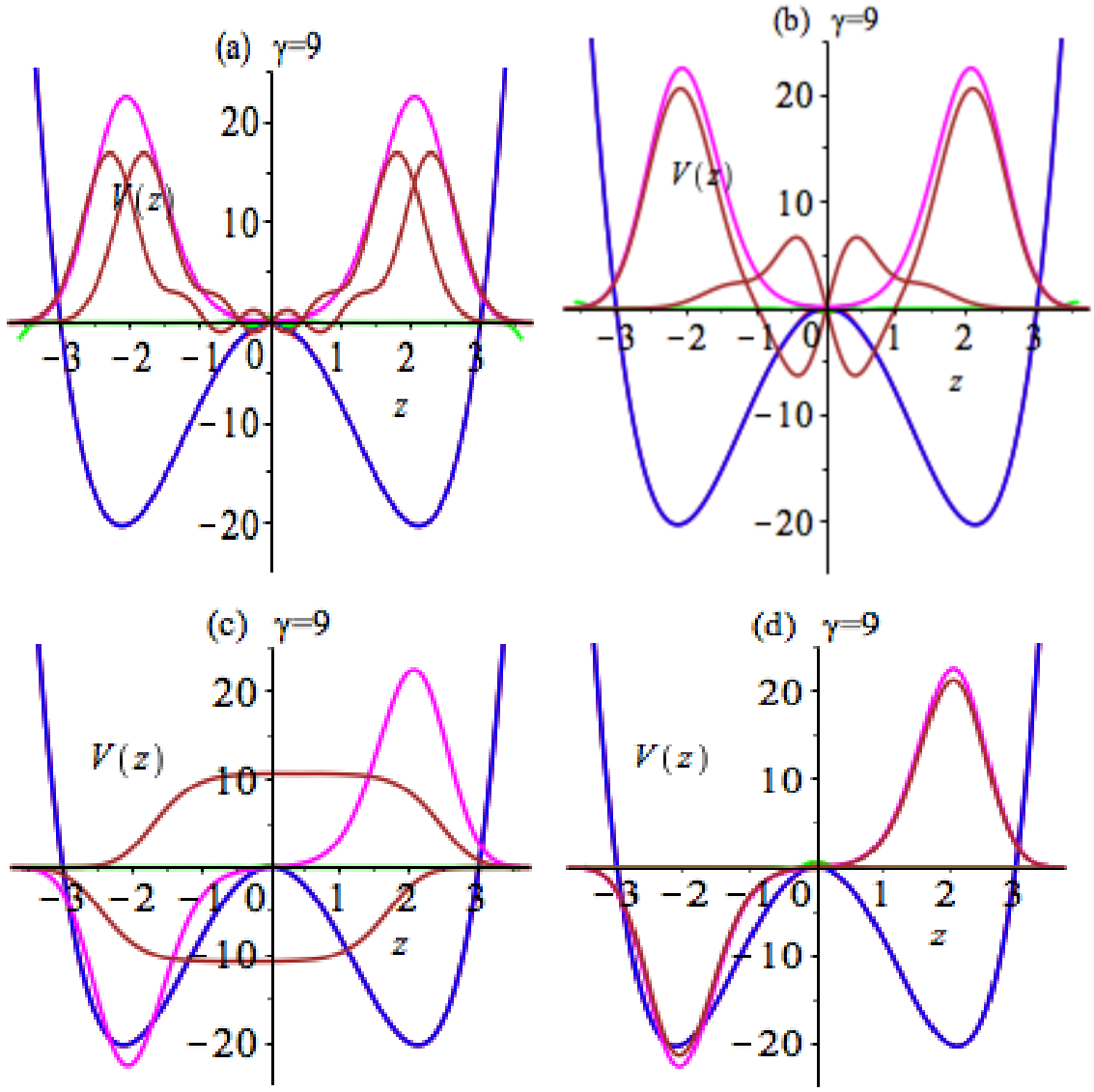
(a) γ=9
V(z)
z
(b) γ=9
V(z)
z
(c) γ=9
V(z)
z
(d) γ=9
V(z)
z

Tables

Table 1. *Ground state energies for three different □ values: first, comparison between the expectation values calculated by using the two-term trial wave functions (Eqn. (4)), and numerical results. Second, the comparison of expectation values calculated from using group A and B wave functions with different numbers of additional terms (columns before the energy values) but equal numbers of variational parameters (middle column). Energy differences are computed with respect to numerical values.*

Ground State (Even Parity)						
γ=3						
Numerical	-0.593493304218	**Difference**				
Variational	-0.571910174548	2.1582559E-02				
Group A		**Difference**	**Parameters**	**Group B**		**Difference**
3	-0.593426761214	6.6543005E-05	5	1	-0.593451727401	4.1576817E-05
6	-0.593493250082	5.4136182E-08	8	2	-0.593492543955	7.6026353E-07
9	-0.593493303802	4.1632198E-10	11	3	-0.593493294373	9.8455760E-09
12	-0.593493304218	2.7000624E-13	14	4	-0.593493304151	6.7342021E-11
γ=6						
Numerical	-5.748190520667	**Difference**				
Variational	-5.678123677177	7.0066843E-02				
Group A		**Difference**	**Parameters**	**Group B**		**Difference**
3	-5.742129052672	6.0614680E-03	5	1	-5.743634202410	4.5563183E-03
6	-5.748166974687	2.3545980E-05	8	2	-5.748172316425	1.8204242E-05
9	-5.748190278821	2.4184573E-07	11	3	-5.748189440448	1.0802196E-06
12	-5.748190517384	3.2832901E-09	14	4	-5.748190517717	2.9500296E-09
γ=9						
Numerical	-16.126186455298	**Difference**				
Variational	-16.094256284192	3.1930171E-02				
Group A		**Difference**	**Parameters**	**Group B**		**Difference**
3	-16.094421450900	3.1765004E-02	5	1	-16.124246020982	1.9404343E-03
6	-16.125772740677	4.1371462E-04	8	2	-16.126164112686	2.2342612E-05
9	-16.126164947436	2.1507862E-05	11	3	-16.126186390164	6.5134000E-08
12	-16.126185938098	5.1720000E-07	14	4	-16.126186451743	3.5548027E-09

Table 2. *First-excited state energies of three different □ values: first, comparison between the expectation values calculated by using the two-term trial wave functions (Eqn. (10)), and numerical results. Second, the comparison of expectation values calculated from using group A and B wave functions with different numbers of additional terms (columns before the energy values) but equal numbers of variational parameters (middle column). Energy differences are computed with respect to numerical values.*

First Excited State (Odd Parity)						
γ=3						
Numerical	0.377662068959	**Difference**				
Variational	0.390215259367	1.2653190E-02				
Group A		**Difference**	**Parameters**	**Group B**		**Difference**
3	0.377678740969	1.6672010E-05	5	1	0.377665058221	2.9892622E-06
6	0.377662122573	5.3614387E-08	8	2	0.377662247886	1.7892739E-07
9	0.377662069225	2.6635300E-10	11	3	0.377662120566	5.1607663E-08
12	0.377662068959	1.3988810E-14	14	4	0.377662069298	3.3923897E-10
γ=6						
Numerical	-5.706792517167	**Difference**				
Variational	-5.665697926927	4.1094590E-02				
Group A		**Difference**	**Parameters**	**Group B**		**Difference**
3	-5.706020074916	7.7244225E-04	5	1	-5.698226913438	8.5656037E-03
6	-5.706746382227	4.6134940E-05	8	2	-5.706787762632	4.7545348E-06
9	-5.706792500726	1.6440860E-08	11	3	-5.706792325598	1.9156866E-07
12	-5.706792517153	1.3860024E-11	14	4	-5.706792513783	3.3835699E-09
γ=9						
Numerical	-16.125958547074	**Difference**				
Variational	-16.094251067076	3.1707480E-02				
Group A		**Difference**	**Parameters**	**Group B**		**Difference**
3	-16.109272519090	1.6686028E-02	5	1	-16.124206033394	1.7525137E-03
6	-16.125780964217	1.7758286E-04	8	2	-16.125953300641	5.2464326E-06
9	-16.125957815272	7.3180150E-07	11	3	-16.125958473483	7.3590499E-08
12	-16.125958542663	4.4106017E-09	14	4	-16.125958542941	4.1327013E-09

REFERENCES

Bardeen, J., Cooper, L. N. & Schrieffer, J. R. (1957). Theory of superconductivity. *Physical Review*, 108, 1175-1204.

Bardeen, J., Cooper, L. N. & Schrieffer, J. R. (1957). Microscopic theory of superconductivity *Physical Review*, 106, 162-164.

Cohen-Tannoudji, C., Diu, B. & Lolöe. F. (1977). *Quantum mechanics*, first edition. Vol. 1 and 2, New York: John Wiley. pp 1148-1155.

DeMille, D., (2015). Diatomic molecules, a window onto fundamental physics. *Physics Today*, December, 34-40.

Feynman, R. P. (1953). Atomic theory of the λ transition in helium. *Physical Review*, 91, 1301-1308.

Feynman, R. P. (1954). Atomic theory of the two-fluid model of liquid helium. *Physical Review*, 94, 262-277.
Feynman, R. P. (1955). Slow electrons in a polar crystal. *Physical Review*. 97, 660-665.
Feynman, R. P. & Cohen, M. (1956). Energy spectrum of the excitations in liquid helium. *Physical Review*, 102, 1189-1204.
Griffiths, D. J. (2005). *Introduction to quantum mechanics*, second edition. Upper Saddle River, NJ: Pearson Preston Hall. Chapter 7 and 8 and the references cited therein.
Gutzwiller, M. C. (1965). Quantized Hall conductivity in two dimensions. *Physical Review A*, 137, 1726-1735.
Hardy, J. R. & Flocken, J. W. (1988). Possible origins of high-Tc, superconductivity. *Physical Review Letters*, 60, 2190-2193.
Hedgahl, E. R., Johnson III, T. L., Schnell, S. E. & Ward, A. R. (2008). Systematic convergence in applying the variational method to the anharmonic oscillator potentials. *Journal of Undergraduate Research in Physics.* 21, http://www.jurp.org/.
Heitler, W. & London, F. (1927). Wechselwirkung neutraler atome und homöopolare bindung nach der quantenmechanik. *Zeitschrift für Physik*, 44, 455-472.
Hylleraas, E. A. (1929). Neue Berechnung der energie des heliums im grundzustande, sowie des tiefsten terms von ortho-helium. *Zeitschrift für Physik.* 54, 347-366.
Hylleraas, E. A. (1963). Reminiscences from early quantum mechanics of two-electron atoms. *Review of Modern Physics.* 35, 421-432.
Hylleraas, E. A. (1970). *Mathematical and theoretical physics*, Vol. II. New York: John Wiley, pp 412-426, and the references cited therein.
Keung, W. Y., Kovac, E. & Sukhatme, U. (1988). Supersymmetry and double-well potentials. *Physical Review Letters*, 60, 41-44.
Koch, J., Schuck, C. & Wacker, B. (2008). Excited states of the anharmonic oscillator problems: variational method. *ibid*, 21, http://www.jurp.org/.
Laughlin, R. B. (1981). Quantized Hall conductivity in two dimensions. *Physical Review B.* 23, 5632-5633.
Laughlin, R. B. (1983). Quantized motion of three two-dimensional electrons in a strong magnetic field. *Physical Review B*, 27, 3383-3389.
Laughlin, R. B. (1983). Anomalous quantum Hall effect: An incompressible quantum fluid with fractionally charged excitations. *Physical Review Letters*, 50, 1395-1398.
Manning, M. F. (1935). Energy levels of a symmetrical double minima problem with applications to the NH_3 and ND_3 molecules. *Journal of Chemical Physics*, 3, 136-138.
Mei, W. N. (1998). Comments on "Phase space integration method for bound states" by Sharada Nagabhushana, B. A. Kagali, & Sivramkrishna Vijay [Am. J. Phys. 65 (6), 563-564, (1997)]. *American Journal of Physics*, 66 (6) 541-542.
Mei, W. N. (1996). Demonstration of systematic improvements in the application of the variational method to harmonic oscillator potentials. *International Journal of Mathematical Education in Science and Technology*, 27, 285-292.
Mei, W. N. (1997). Combined variational-perturbative approach to the anharmonic oscillator problems. *International Journal of Mathematical Education in Science and Technology*, 28, 495-511.
Mei, W. N. (1998). Combined variational-perturbative approach to the anharmonic oscillator problems. *International Journal of Mathematical Education in Science and Technology*, 29, 875-893.
Mei, W. N. (1999). Demonstration of systematic improvements in the application of the variational method to weakly bound potentials. *International Journal of Mathematical Education in Science and Technology*, 30, 513-540.
Merzabacher, E. (1961). *Quantum mechanics*, first edition. New York: John Wiley. pp 393-396.

Ninemire, B. & Mei, W. N. (2004). Demonstration of systematic improvements in the application of the variational method to strongly bound potentials. *International Journal of Mathematical Education in Science and Technology*, 35, 565-583.

Razavy, M. (1979). An exactly soluble Schrödinger equation with a bistable potential field. *American Journal of Physics*, 48, 285-288. Ronveaux, A. (1995). *Heun's differential equations*. Oxford: Oxford University Press.

Schiff, L. L. (1968). *Quantum mechanics*, third edition. New York: McGraw-Hill. pp 255-262.

Slavyanov, S. Y. & Lay, W. (2000). *Special functions, a unified theory based on singularities.* Oxford: Oxford Mathematical Monographs.